Uniform π-System Alignment in Thin Films of Template-Grown Dicarbonitrile-Oligophenyls

ARTICLE *in* ADVANCED FUNCTIONAL MATERIALS · MAY 2011

Impact Factor: 11.81 · DOI: 10.1002/adfm.201001940

13 AUTHORS, INCLUDING:

F. Klappenberger
Technische Universität München
79 PUBLICATIONS **1,742** CITATIONS
SEE PROFILE

Alexei Nefedov
Karlsruhe Institute of Technology
107 PUBLICATIONS **1,106** CITATIONS
SEE PROFILE

Thomas Strunskus
Christian-Albrechts-Universität zu Kiel
194 PUBLICATIONS **3,113** CITATIONS
SEE PROFILE

Christof Wöll
Karlsruhe Institute of Technology
551 PUBLICATIONS **17,514** CITATIONS
SEE PROFILE

Uniform π-System Alignment in Thin Films of Template-Grown Dicarbonitrile-Oligophenyls

Florian Klappenberger, Dirk Kühne, Matthias Marschall, Stefan Neppl, Wolfgang Krenner, Alexei Nefedov, Thomas Strunskus, Karin Fink, Christof Wöll, Svetlana Klyatskaya, Olaf Fuhr, Mario Ruben, and Johannes V. Barth*

The ordering and conformational properties of dicarbonitrile-para-oligophenyls are studied with complementary methods, namely X-ray structure analysis, low-temperature scanning tunneling microscopy, and near-edge X-ray absorption fine-structure spectroscopy. The packing of the functionalized variants differs from their technologically interesting para-oligophenyl counterparts, both in the bulk crystal phase and in thin films grown by organic molecular beam epitaxy (OMBE) under ultra-high vacuum conditions on the Ag(111) surface. In the crystal phase, the conformation depends on the number *n* of phenyl rings, exhibiting an intriguing screw-like structure in the case of *n* = 4 at room temperature as well as at 180 K. For OMBE-grown thin films, the whole series acquires the same type of conformation, characterized by alternately twisted phenyl rings, similar to the pure oligophenyl species. However, for all tested molecules, the orientation of the molecular reference plane is uniform within the entire film and coincides with the surface plane. This contrasts with the herringbone ordering adopted by the phenyl backbones without the carbonitrile groups. Our results demonstrate how the functionalization of moieties with extended conjugated electron systems can help to improve the structural homogeneity in technologically relevant organic thin films.

1. Introduction

Thin films of para-oligophenyl (Ph_X) molecules have attracted widespread interest due to their appealing optical and electronic properties.[1] In particular, they were successfully used as active layers in organic thin film transistors[2] or in organic light-emitting devices.[3,4] The optical characteristics of the single molecules are highly anisotropic[5] and allow for the emission of linearly polarized light.[6] Since, in the final device, a large ensemble of molecules is present, its performance depends strongly on the degree of ordering in the active layer.[7] Thus, to tune the properties of the resulting applications, it is important to have the means to control both the azimuthal as well as the rotational order in organic thin films. Several different methods have been employed so far to control the orientation of oligophenyl layers. A uniform azimuthal orientation can be imposed on the thin film by rubbing a precursor layer linearly[8] or by growth on anisotropic substrates.[9–11] In contrast, no efficient ways to control the rotation of the molecular plane (defined as the reference plane later on in the text) around the long molecular axis are known. In the bulk, the planes of two neighboring molecules include an angle of 66°,[12–14] an arrangement further referred to as the herringbone ordering. For thin films grown on insulating[14] as well as on noble metal surfaces,[8,15,16] very similar ordering was reported by the different research groups.

From a general perspective, for several types of molecules, the influence of template-growth on organic thin films has been investigated. For perylene[17,18] and pentacene,[19–21]

Dr. F. Klappenberger, D. Kühne, M. Marschall, S. Neppl, W. Krenner, Prof. J. V. Barth
Physik Department E20, TU München, James-Franck Str. 1
D-85748 Garching, Germany
E-mail: fklapp@ph.tum.de
Dr. T. Strunskus
Christian-Albrechts-Universität Kiel
Kaiserstr. 2, D-24143 Kiel, Germany
Dr. A. Nefedov, Prof. C. Wöll
Institut für Funktionelle Grenzflächen (IFG)
Karlsruher Institut für Technologie (KIT)
Hermann-von-Helmholtz-Platz 1
D-76344 Eggenstein-Leopoldshafen, Germany
Dr. K. Fink, Dr. S. Klyatskaya, Dr. O. Fuhr, Prof. M. Ruben
Institut für Nanotechnologie (INT)
Karlsruher Institut für Technologie (KIT)
Hermann-von-Helmholtz-Platz 1
D-76344 Eggenstein-Leopoldshafen, Germany
Dr. M. Ruben
Institute de Physique et Chimie de Matériaux de Strasbourg (IPCMS)
CNRS-Université de Strasbourg
67034 Strasbourg, France

DOI: 10.1002/adfm.201001940

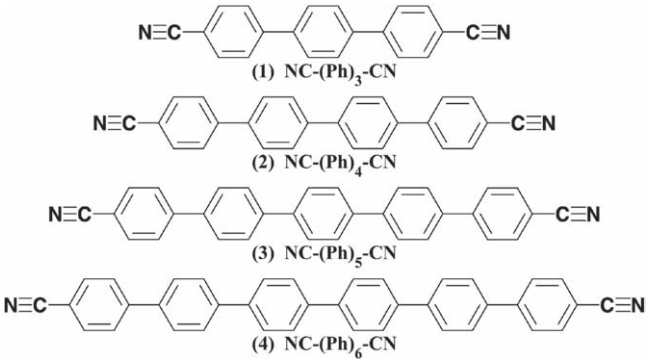

Scheme 1. Dicarbonitrile-oligophenyl molecules **1** to **4** used in this study.

the ordering of the first monolayers depends strongly on the underlying substrate but for thick enough multilayer films, a bulk-like structure prevails.[22,23] For molecules with stronger intermolecular forces due to functional groups like perylene-tetracarboxylic-dianhydride[24] or biphenyl-oxalic amide,[25] the transition to the bulk ordering takes place even faster. The use of strongly corrugated substrates such as Cu(110) and its oxygen-covered variant allowed controlling the azimuthal alignment of sexithiophene[26] and the afore mentioned sexiphenyl,[9] but in both cases only minor changes to the bulk-like ordering could be achieved in the thin films. Only in rare cases did the substrate-induced ordering persist in multilayer films. For example, supramolecular columns of hexabenzocoronenes can be grown on Cu(111) and Au(111) surfaces, featuring completely different packing compared to the herringbone bulk structure.[27]

Here, we study the conformation and orientation properties of functionalized variants of oligophenyl molecules, namely dicarbonitrile-oligophenyl molecules (**Scheme 1**) in bulk and thin films of varying thickness grown on the Ag(111) surface. In the thin films produced by organic molecular beam epitaxy (OMBE), both quantities differ drastically from the bulk structure. The conformation deviates from a planar conformation by alternatively left and right rotated phenyl rings. The orientation of the molecules' reference planes is uniform throughout the whole film. The latter is in contrast to the wellknown herringbone ordering of the pure unfunctionalized oligophenyl species. The novel ordering not only appears in the special case of a single species, but systematically for all four representatives of the examined series. We attribute the improved homogeneity of the multilayer films to the high-quality template formed by the first adsorbed monolayer of the functionalized species in combination with the increase of the molecule–molecule interaction due to the functionalization. Our method of specifically tuning the molecule–substrate ordering as well as the intermolecular forces by adequate extension with functional groups provides a novel way to tune the properties of organic thin films.

2. Results and Discussion

In a three-dimensional (3D) layer the geometry of a single molecule is characterized by a set of angles. For the following

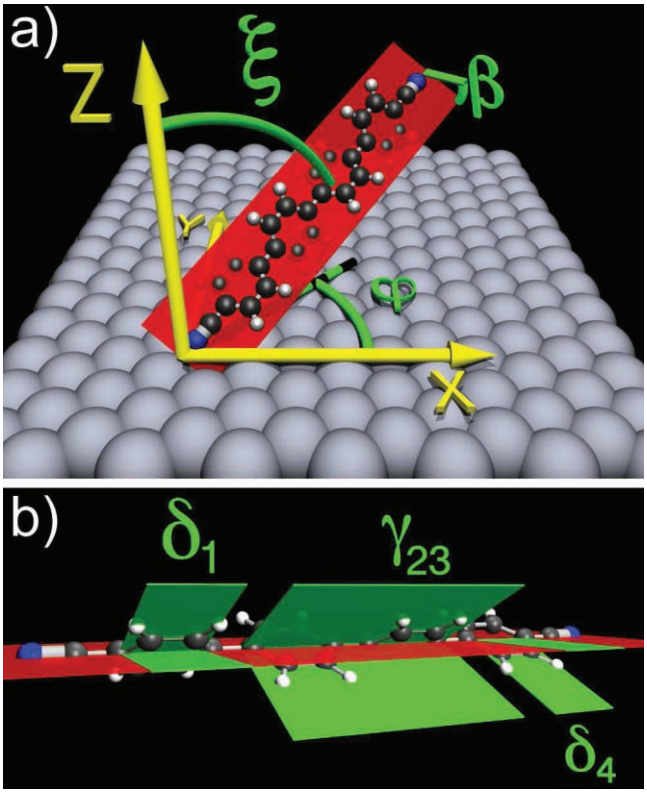

Scheme 2. Definition of the angles characterizing a) the molecular orientation by the angles ξ, φ, and β and b) the conformation by the angles δ_n and γ_{nm} in thin film samples.

discussion we reference the orientation and the conformation of the NC–Ph$_x$–CN species as defined in **Scheme 2**. The main axis of the molecule, from nitrogen to nitrogen, has an angle ξ with the surface normal and an azimuth angle φ with an arbitrarily defined x-axis chosen along the [–1–12]-direction of the crystal (Scheme 2a). Since the phenyl rings can rotate around the connecting σ-bonds, we need a system to describe the multitude of possible conformations. As reference plane, we define the plane to which all phenyl rings would be aligned if they were coplanar (Scheme 2a, transparent red). The tilt of this reference plane with respect to the substrate is characterized by the angle β. Non-planar conformations of the molecule result from a rotation of the phenyl rings (n = 1 to 4) are accounted for by the angles δ_n (Scheme 2b) defined as clock-wise rotation around the main axis when looking along the latter. Accordingly, the twist angle between two adjacent phenyl rings n and m amounts to $\gamma_{mn} = \delta_n - \delta_m$ and specifies the angle one has to rotate ring m around the main axis to be coplanar with ring n again in clock-wise manner with the view along the main axis. The situation displayed in Scheme 2a is defined by $\xi = 60°$, $\varphi = 45°$, $\beta = 40°$, $\delta_1 = \delta_3 = -25°$, $\delta_2 = \delta_4 = +25°$, $\gamma_{12} = \gamma_{34} = 50°$, and $\gamma_{23} = -50°$.

For the determination of the orientation of the oligophenyl backbone and the conformational properties within the thin films, we use angle-dependent near-edge X-ray absorption fine-structure (NEXAFS) spectroscopy. NEXAFS is sensitive to the adsorption angle α of a specific molecular moiety (as defined

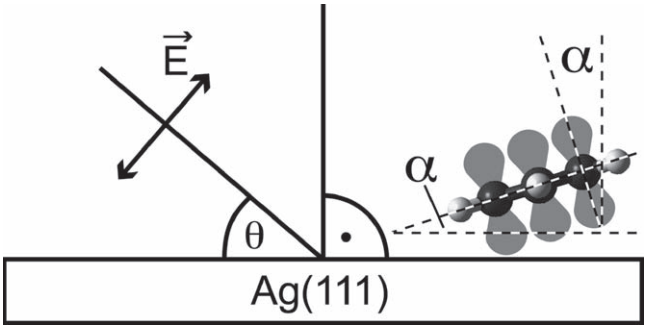

Scheme 3. The geometry of the NEXAFS setup. The incidence angle θ defines the direction of the X-ray beam with respect to the sample surface. The adsorption angle α describes the orientation of a molecular moiety with respect to the underlying surface. In the displayed example of a benzene ring (carbon atoms in black, hydrogen atoms in white), α is the angle between the direction of the π-system (gray lobes) and the surface normal.

in **Scheme 3**), because the detected intensity depends on the corresponding angle between the E-vector of the X-ray beam and the direction of the specific final state molecular orbital.[28] In our samples, at least 3-fold azimuthal symmetry is present, thus the theoretic NEXAFS curves for different α cross in a single point (as shown in the Supporting Information, Figure S1) defining the magic angle. In our setup (Scheme 3), the incidence angle θ of the X-ray beam can be adjusted from near-grazing incidence ($\theta = 25°$) to normal incidence ($\theta = 90°$) by rotation of the sample. In the exemplary case of a π^* resonance of a planar ($\alpha = 0°$) benzene ring, we obtain strongest and vanishing intensity for grazing and normal incidence, respectively. Since a distinct angle α can result from various molecular geometries (sets of ξ, β, δ), making conclusions about the ordering in a thin film only from α is nontrivial and requires additional information. As will be demonstrated below, the shape of the first π^* resonance of the phenyl rings depends sensitively on the twist angle γ and can thus provide such information.

2.1. Crystal Structures

In order to compare the crystal phase conformation and packing of solid Ph_X and NC–Ph_X–CN (Scheme 1) we applied X-ray structure analysis. Single crystals of **1** and **2** suitable for X-ray diffraction analysis were obtained by slow evaporation of the solutions in chloroform and 1,4-dioxane, respectively. Due to low solubility in all common organic solvents, it was not possible to obtain single crystals of **3** and **4** suitable for X-ray diffraction. The data were obtained at 180 K. Chemically equivalent bond lengths and angles agreed within the experimental error.

The compound **1** crystallizes in the monoclinic space group $P2_1/n$ with two molecules per unit cell. The 3D visualization of the conformation (**Figure 1**a) highlights that the central phenyl ring is rotated out of the plane of the two terminal rings. The two dihedral angles between adjacent rings both amount to 31.56 (5)°. The anisotropic displacement ellipsoids and atom labeling are shown in Figure SI2a. The molecules arrange in layers parallel to the (10–2)-plane (red line, Figure 1b). Within this plane, chains appear that follow the projection of direction **c**

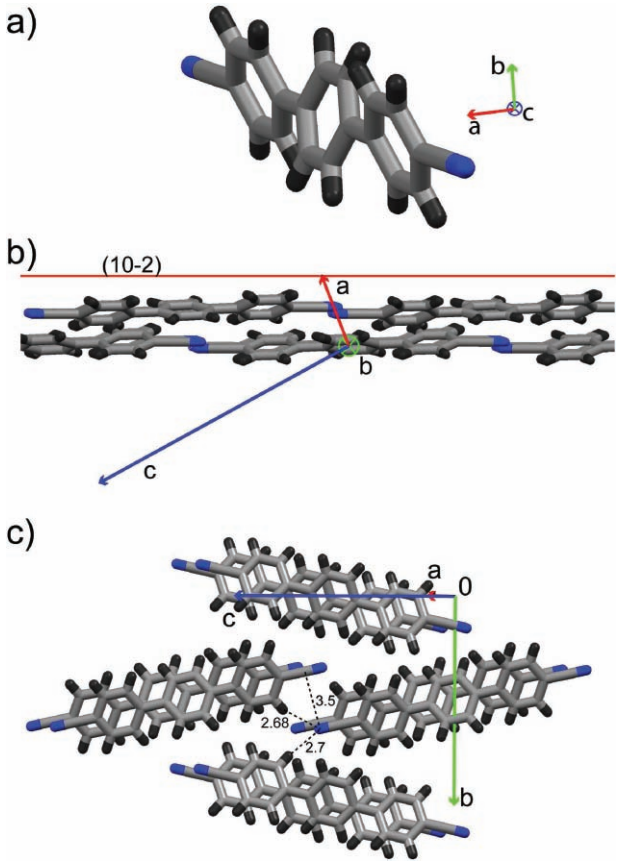

Figure 1. The crystal structure of **1** (NC–Ph_3–CN) as obtained by X-ray structure analysis. a) 3D visualization of the molecular conformation (view along direction *c*, blue = nitrogen, gray = carbon, black = hydrogen). b) Molecules arrange in layers parallel to the (10–2)-plane (red line). c) CN groups acquire an anti-parallel ordering motif. The two shortest H bonds (of the N···HC type) are highlighted. All distances are given in Å.

onto this plane (central two molecules in Figure 1c). The chains feature an anti-parallel CN–CN motif with a distance from center to center of CN-groups of 3.50 Å. This binding motif is similar to the one observed for 4,4′-dicarbonitrile-biphenyl,[29] for which the corresponding distance is 3.55 Å. Within the solid phase of compound **1**, the shortest CH···N hydrogen bond distances amount to 2.68 Å and 2.70 Å (N···H separation). Again the values closely resemble the ones from NC–Ph_2–CN. Thus we follow the argumentation of Britton et al.[29] and conclude that the chain formation of NC–Ph_3–CN results from a combination of dipole–dipole interaction and H bonding. The different layers stack in molecular columns oriented along the *a*-axis with identical arrangement of the individual moieties resulting in a π-stacking distance of 3.69 Å and the lateral offset of approximately half a phenyl ring along the main axis, as can be seen in Figure 1b, typically appearing for π-stacking.[30–32]

The X-ray structure analysis of compound **2** is summarized in **Figure 2**. Again, crystallization takes place in a monoclinic system, but this time in space group C2/c with four molecules per unit cell. All four molecules exhibit the same conformation (Figure 2a) characterized by a gradual rotation of the phenyl rings resulting in a screw-like structure. The anisotropic

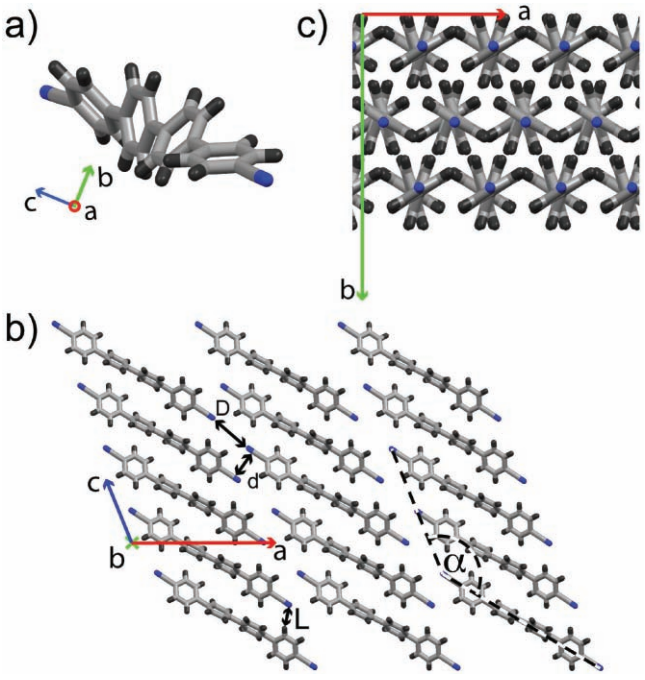

Figure 2. The crystal structure of **2** (NC–Ph_4–CN) as obtained by X-ray structure analysis. a) 3D visualization of the screw-like conformation. (blue = nitrogen, gray = carbon, black = hydrogen) b) In the *ac*-plane chains are formed with separation *d* between neighboring anti-parallel CN groups and distance *D* for opposing CN groups. c) Sheets of molecules appear in a certain direction of the crystal, but no direct stacking of identically oriented molecules as in the NC–Ph_3–CN case is possible due to the intricate screw-like conformation.

displacement ellipsoids and atom labeling are shown in the SI in Figure SI2b. The dihedral angles between the two peripheral adjoining rings are 40.00 (5)° on both sides. Between the two central adjoining rings the angle amounts to 33.52 (6)° leading to a rotation of the last phenyl ring of 113.52 (5)° against the first one. The long axis of the molecule is distorted such that the carbon atoms connecting the phenyl rings deviate from the straight line connecting the terminal nitrogen atoms. Similar distortions are quite common for molecules with aromatic rings connected in para position.[29,33,34] A slice parallel to the *ac*-plane (Figure 2b) demonstrates that the molecules of **2** are arranged in rows along the *c*-direction of the unit cell. The angle α between the row direction and the direction of the long molecular axis (Figure 2b, black and white dashed lines) amounts to $\alpha = 142°$. The antiparallel arrangement of the carbonitrile groups with the shortest distance *d* (3.58 Å from center to center) indicates an attractive interaction due to the dipolar character of the terminal group. Following the long molecular axis of one molecule an opposing carbonitrile group can be found oriented such that a repulsive interaction would be expected. However, the distance *D* between these functional groups amounts to 6.4 Å, thus the corresponding repulsive energy is negligible (Figure 2b). Each nitrogen atom establishes two CH···N hydrogen bonds, one connecting to the neighboring molecule within the layer (displayed in Figure 2b) with a N···H separation *L* of 2.75 Å and one connecting to a molecule of the next layer (not displayed) with the separation of 2.73 Å. As can be seen in Figure 2c, a layer-by-layer arrangement is present in the crystal phase, but no direct stacking of identically oriented molecules as in the NC–Ph_3–CN case takes place. The shortest distance between phenyl rings of adjacent molecules that could possibly lead to π–stacking adds up to 4.6 Å, suggesting only minor contribution to the crystal structure formation.

The similarity of the distances for dipole–dipole interaction and for hydrogen bonding in the three cases (NC–Ph_2–CN, NC–Ph_3–CN, NC–Ph_4–CN) indicates that the carbonitrile groups are a decisive factor for the packing of this type of molecules. Furthermore, the influence of the functional groups on the packing is not reduced by the extension of the phenyl backbone despite the decrease of the ratio of CN groups with respect to phenyl groups.

At this point, it is interesting to compare with a asymmetrically functionalized oligophenyl. Recently, it was shown that para-carbonitrile-quaterphenyl packs in a herringbone pattern with layers of upright standing molecules.[35] In the unit cell, two molecules are present with antiparallel orientation with respect to the position of the carbonitrile group. This indicates that the presence of CN groups on both ends of the stick-like organic species are required to sufficiently influence the crystal packing and overcome the herringbone alignment.

We have aimed to also characterize the NC–Ph_4–CN crystal structure with NEXAFS, as a reference to which the NEXAFS measurements of the later sections can be compared. We prepared a film by pressing and smearing powder consisting of several hundred micrometer long crystallites onto a conductive glue tape. Unfortunately, no reasonable signal could be obtained due to charging effects of the sample.

2.2. OMBE-Grown Thin Films at Low Temperature

As a next step, we have grown thin films of molecule **2** by OMBE onto the Ag(111) surface with thicknesses ranging from half a monolayer to approximately 20 monolayers (ML), where a ML is defined as a saturated densely-packed layer with all the molecules adsorbed flat on the substrate.[36] The OMBE was conducted using a Knudsen-type cell with a quartz crucible holding the organic material. A multilayer film of molecule **2** was grown by 150 min evaporation of NC–Ph_4–CN with the crucible held at 270 °C and a substrate temperature between 160 and 220 K. The substrate was cooled to increase the sticking coefficient of the organic molecules and to reduce beam damage during exposure.[37] From the height of the absorption step, a layer thickness of approximately 20 ML was calculated, taking into account a mean free path corresponding to the thickness of five organic ML. This is in good agreement with published values[38] for inelastic mean free paths in quaterphenyl films for electrons with a kinetic energy of 300 eV. The NEXAFS spectra of the multilayer film (**Figure 3**) show a strong dichroism in both measured regions, namely the C1s and the N1s region, indicating the presence of a high degree of molecular orientation. The π^* region of the carbon edge (Figure 3a) is dominated by the typical[16,39,40] strong phenyl ring resonance at 285.1 eV and a second sharp feature almost two eV higher. Two broader peaks are discernible around 288.7 and 290.2 eV before the σ^* region begins with its first peak at 293 eV. A zoom into the π^* region

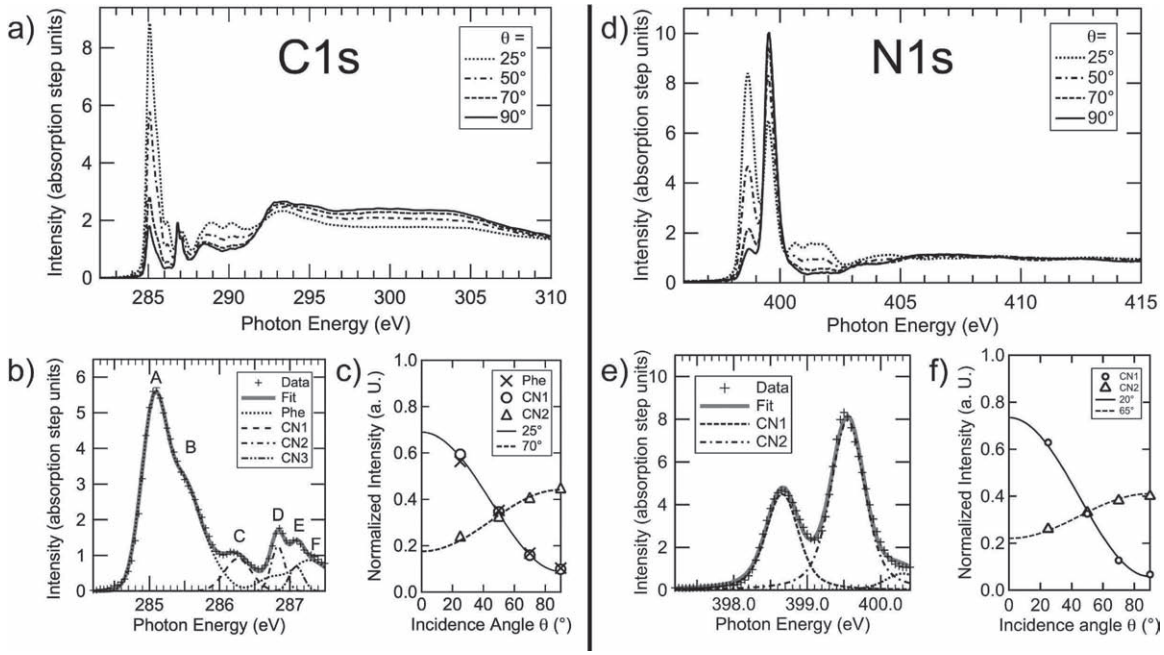

Figure 3. NEXAFS data and analysis of a sample with more than 20 ML of NC–Ph_4–CN on Ag(111). a) Angle-dependent C1s spectra. b) Zoom of the C1s leading edge showing the fit (solid line) to the experimental data (crosses) and the different spectral constituents (dashed lines). c) The angle dependence of the peaks of interest (symbols) with theoretical curves (lines). d) Angle-dependent N1s spectra. e) Zoom of the N1s leading edge showing the fit (solid line) to the experimental data (crosses) and the different spectral constituents (dashed lines). f) The angle dependence of peaks of interest (symbols) with theoretical curves (lines).

(Figure 3b) reveals that, in addition to the spectral part originating from the phenyl rings (peaks A, B, and F, dotted line), additional resonances (peaks C, D, and E, dashed and dash-dotted lines) are present in the spectrum which are absent in the spectra of benzene or oligophenyl.[16,39,40] We attribute the additional resonances to excitations into orbitals related to the two perpendicular π bonds of the carbonitrile groups. The π orbital oriented perpendicular to the adjacent phenyl ring will be further referred to as "out-of-plane"; that which is oriented within the plane of the phenyl ring is accordingly denominated "in-plane". In order to determine the orientation and conformation of the molecules, we analyze the angle dependence of peaks A, C, and D (Figure 3c), which provide the orientation of the conjugated π system of the phenyl rings (Phe) and the terminal group (CN1 and CN2). The best fit is obtained for theoretic curves according to an angle α of 25° (solid line) for the phenyl rings (peak A) as well as for the out-of-plane carbonitrile π^* orbital (peak C) that is hybridizing with the backbone[41] and an angle α of 70° for the perpendicular-oriented in-plane π^* resonance (peak D). These two angles (25° and 70°) result from independent fits and agree with the perpendicularity of the respective orbitals within the experimental error of approximately 5°.

In analogy to the carbon region, the N1s data are presented in Figure 3d–f. Two strong π^* resonances dominate the spectra (Figure 3d) and can again be attributed to the two perpendicular π^* orbitals of the carbonitrile groups. According to density-functional theory calculations,[41] the energetically lower-lying out-of-plane orbital (398.7 eV) is hybridized with the conjugated π system of the phenyl rings, while the in-plane orbital (399.7 eV) does not take part in that interaction. The range between 400 eV and 403.5 eV shows more and overlapping resonances than in the benzonitrile case.[41] Based on our preliminary results of density-functional theory calculations, we attribute the increase in resonances to the higher number of phenyl rings and the second carbonitrile group. A detailed analysis of the assignment will be published elsewhere.[42] The σ^* transitions (403.5 eV and higher) show very small oscillator strengths. For a further test of the molecular adsorption geometry obtained from the C1s data, we again evaluate the angle dependence quantitatively and focus on the sharp resonances at the leading edge (Figure 3e) to fit the experimental data (+ symbols) with Voigt peaks (CN1 and CN2). The analysis (Figure 3f) indicates $\alpha = 20°$ for the out-of-plane orbital (CN1) and $\alpha = 65°$ for the in-plane orbital (CN2). Thus both the C1s data and the N1s data agree well within the experimental error.

For the interpretation of these angles we first review the crystal packing featuring four differently oriented phenyl rings resulting in the screw-like conformation. A simple calculation taking into account this conformation shows that in the bulk phase for the phenyl rings an average NEXAFS angle $\alpha \sim 45°$ would result, only slightly depending on the overall orientation (assumed tilt angle β). Furthermore, Müllegger et al. measured OMBE grown thin films of quaterphenyl and found a significantly less pronounced dichroism compared to our case.[16] The authors showed that such a weak angle-dependence is consistent with the typical herringbone packing of oligophenyl molecules. Comparison of these two cases shows that the pronounced dichroism in the spectra of the OMBE grown NC–Ph_4–CN multilayer sample must originate from a novel molecular packing.

Since NEXAFS spectroscopy is sensitive to both the ring twist angle γ and the orientation angle β (cf. Scheme 2), but measures only one averaged angle, it is nontrivial to determine the packing from the angular dependence of the NEXAFS resonance intensities. In the following we will disentangle the combined information by first focusing on the conformation, mainly governed by the twist angles γ, and then analyzing the alignment of the molecular reference planes characterized by β.

As pointed out in an earlier publication, for systems containing phenyl-rings, information on the twist angle γ between adjacent phenyl rings can be obtained from an analysis of relative resonance intensities within a NEXAFS-spectrum recorded for the magic angle.[43] In order to make such an analysis possible, we carried out a series of ab-initio simulations of NEXAFS spectra of NC–Ph_4–CN using the commercial program package StoBe.[44] The simulations included the C1s as well as the N1s region and successfully described both, as will be detailed in a forthcoming publication.[45] The calculated spectra correspond to magic angle spectra and do not take into account any information on the molecular orientation, thus ξ, φ, and β are irrelevant for these spectra. Here, we focus on the low-energy part of the NEXAFS spectra showing the two lowest C1s–π^* excitations into the lowest unoccupied molecular orbital (LUMO) and the LUMO+1. The curves presented in **Figure 4**a were calculated for molecules with different conformations, characterized by the different twist angles γ from 0° to 60°. We assumed a symmetric left-right rotation through $\delta = \pm \gamma/2$ of neighboring phenyl rings as visualized in Scheme 2. The results clearly demonstrate that the relative intensity of the two components contained in this bimodal part of the data is very sensitive to the twist-angle γ between the phenyl-rings. In other words, the shape of the magic angle curve allows us to determine geometrical aspects of the molecular conformation, which is typically not possible with NEXAFS. Here, each of the calculated spectra consists of a superposition of a total of 12 excitations from 9 non-equivalent C1s-initial states, each convoluted with a Gaussian (FWHM 0.4 ± 0.1 eV). The high sensitivity to the molecular geometry results from a twist angle dependent variation of the electronic coupling of the different carbon initial states (on- vs off-axis carbon atoms) with the final state π–systems. Such a sensitivity was already successfully used in the analysis of self-assembled monolayers of pyridine-terminated thiolates on gold.[43] A more detailed discussion of the microscopic origins of this dependence will be presented in the afore-mentioned forthcoming publication.[45]

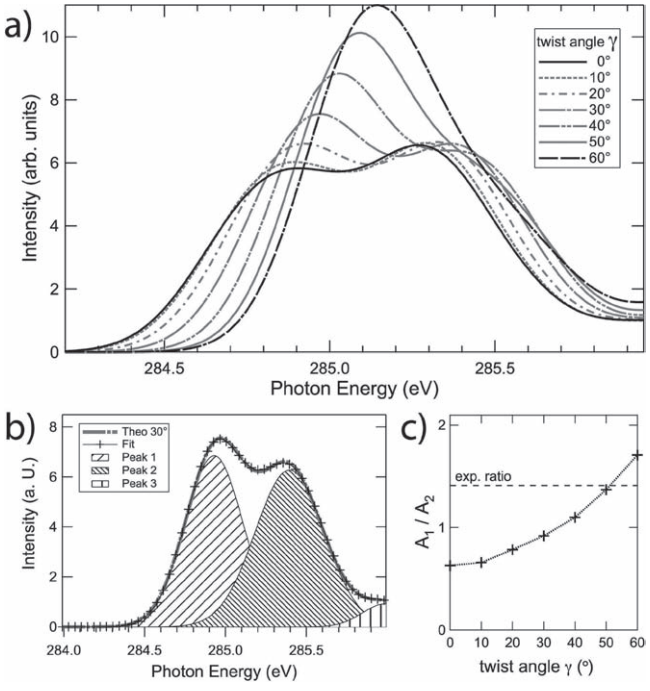

Figure 4. Theoretic investigation of the correlation between the twist angle γ and the shape of the phenyl ring related NEXAFS resonance at 285 eV. a) Simulated NEXAFS spectra show a pronounced shape dependence on the assumed molecular conformation characterized by γ. b) Example of the fitting procedure determining the ratio of the areas of the peaks 1 and 2. c) The theoretic curve correlating the conformation of a molecule (described by the twist angle γ) with a certain ratio of the areas of the first to peaks (A_1/A_2). The dotted line reflects the experimental value of A1/A2 as obtained from the fit in Figure 5. The crossing of the two curves indicates an experimental twist angle of $\gamma = 50°$.

In order to enable a simple determination of the experimental twist-angle we subjected each of the simulated spectra to a fitting-procedure. The fits (Figure 4b, example for $\gamma = 30°$) were carried out using three Gaussians corresponding to the excitations into π^*1 (Peak 1), π^*2 (Peak 2) and an additional background. Then, the ratio A_1/A_2 of the areas of Peaks 1 and 2 was calculated for each value of γ.

The corresponding theoretic curve (Figure 4c, dotted line) thus correlates the shape of the phenyl related resonance with the molecular geometry. Next, we fit the experimental magic angle spectrum in the same fashion as the theoretic spectra (**Figure 5**). The experimental ratio A_1/A_2 amounts to 1.37. Drawing a constant line with this value in Figure 4c, the crossing with the theoretic curve indicates that the experimental twist angle γ is close to 50°.

Knowing the twist angle γ the interpretation of the average adsorption angle α_{aver} becomes quite clear. The only possibility

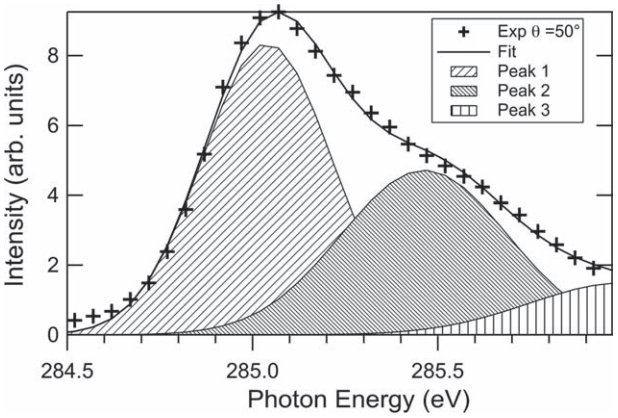

Figure 5. Evaluation of the experimental twist angle. The shape of the experimental magic angle curve for the multilayer of molecule **2** (plus symbols) was subjected to the same fitting procedure as the calculated curves of Figure 4. The experimental data can well be approximated (solid line) by three Gaussian peaks. The ratio of the area of the first two peaks A_1/A_2 amounts to 1.37 and indicates an experimental twist angle γ_{exp} = 50° by the crossing with the theoretic curve (Figure 4c).

to obtain $\alpha_{aver} = 25°$ is that the molecular reference planes of all molecules must be aligned in one plane coplanar to the surface ($\xi = 90°$, $\beta = 0°$). Then having half of the phenyl rings with $\delta = 25°$ and the other half with $\delta = -25°$, the resulting twist angles are $\gamma = 50°$ and $\alpha_{aver} = 25°$ (cf. Scheme 2). Note, that due to the non-trivial trigonometric integration, which the NEXAFS signal is based on, the intuitive solution with half of the phenyl rings planar and half of them rotated by 50° ($\beta = 25°$, $\alpha = 0°/50°$) would result in $\alpha_{aver} = 33°$ (see Figure SI2) and can thus be ruled out.

Now we compare the packing of oligo-phenyl molecules with our functionalized variants. Experiment and theory agree that in para-oligo-phenyl molecules adjacent phenyl rings always feature a ring twist angle γ (**Figure 6**, left panel) which varies from 20° to 50° depending on the individual study.[13,16,46–51] In contrast, planar conformations appear only if sufficiently strong external forces like mechanical pressure change the double-well potential for the ring rotation into a single-well potential.[52,53] Thus, the functionalization leaves the twist untouched, but changes the packing from a herringbone type, where neighboring molecules exhibit tilted planes ($\Delta\beta = 66°$), to a uniform alignment in which all molecules have their reference planes oriented planar with the surface ($\beta = 0°$). A schematic drawing of the molecular arrangement is given in Figure 6, right panel. In addition the ordering present in the NC–Ph_4–CN multilayer must be extremely regular, because deviations with positive and negative angle do not cancel out in NEXAFS, so the average value for α would be increased to more than $\beta/2$.

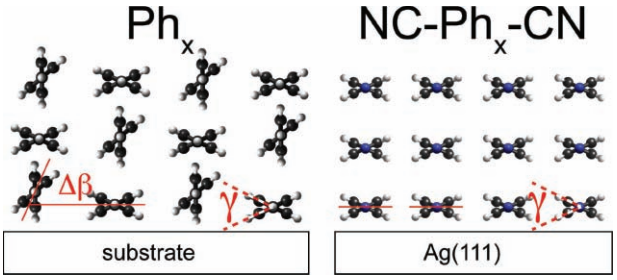

Figure 6. Comparison of thin film ordering between oligophenyls (left panel) and para-dicarbonitrile-oligophenyls (right panel). The direction of the view is along the main axis of the molecules (C, H, N atoms displayed with black, white, and blue spheres, respectively). In the herringbone packing exhibited by oligophenyl molecules on the different substrates the average molecular layers (red lines) of adjacent molecules are rotated by $\Delta\beta \sim 66°$, while the packing of the dicarbonitrile variants feature $\beta = 0°$ (red lines) for all molecules. The ring twist angle γ remains untouched by the functionalization.

In **Figure 7**, we compare the spectra of thin film samples of molecules **1**, **3**, and **4** (Figures 7a, b, and c, respectively). The thickness of the films amounts to approximately 20 ML. The overall resonance structure is very similar, as one might expect for a series of one type. The only systematic change occurs for the double peak at 287 eV, which decreases with increasing number of phenyl rings. This decrease is a further confirmation of our assignment of these resonances to the carbonitrile group, since with a higher number of phenyl rings the relative

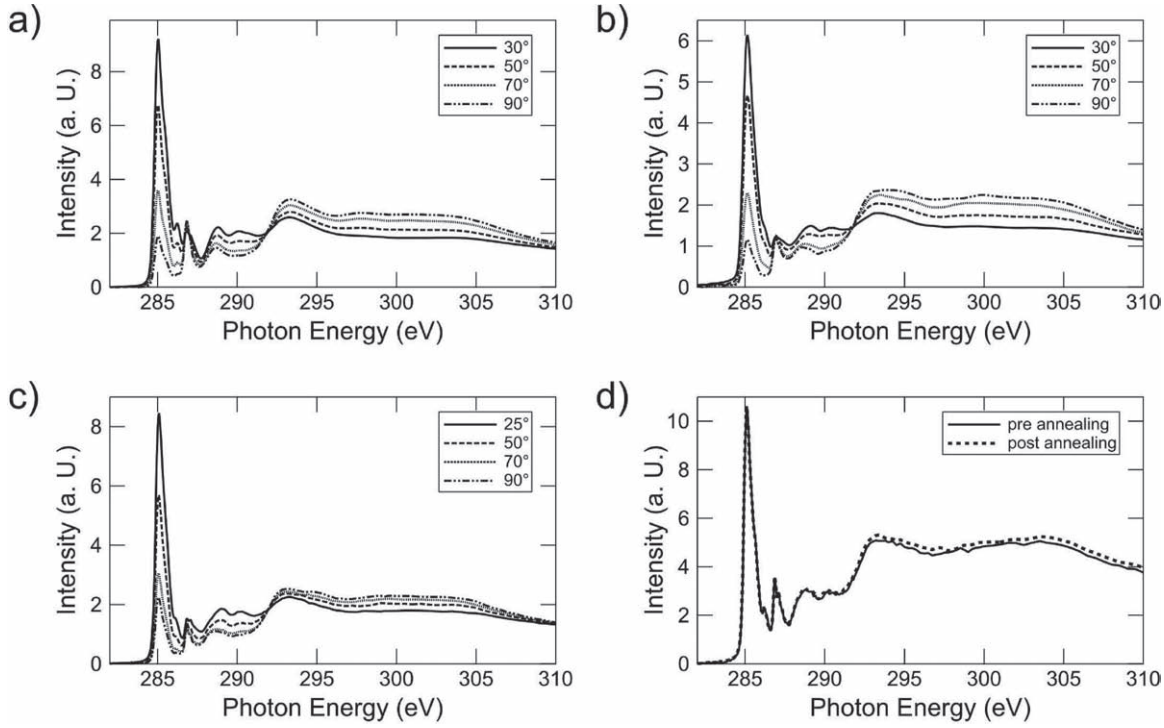

Figure 7. a), b), c) C1s NEXAFS spectra for molecules **1**, **3**, and **4** showing very similar angle dependence as the spectra for molecule **2** indicating that the template effect is influencing the thin film growth for the whole molecule class. d) C1s NEXAFS spectra of a thin film of **2** ($\theta = 25°$) before and after annealing to 300 K demonstrate the room-temperature stability of the thin film grown at low-temperature (~160 K).

intensity of the CN resonances is expected to diminish. The same type of analysis of the shapes and the angle dependences of the leading π^* region, as the one which has been carried out for molecule **2**, indicates similar values ($\alpha = 25°$, $\gamma = 50°$, $\beta = 0°$) also for molecules **1**, **3** and **4**.

We conclude that the template-induced uniform ordering of dicarbonitrile-oligophenyls is a general effect in this class of molecules and not only occurring for a special molecular species. For the entire series, the thin films are characterized by a twisted ring conformation ($\gamma \sim 50°$) and a high degree of uniform alignment of the molecular reference planes ($\beta \sim 0°$).

We have tested the room-temperature stability of the well-ordered multilayer films. The comparison of spectra (measured at 160 K, *not* normalized to the edge jump) for $\theta = 25°$ before and after annealing a multilayer of molecule **2** to 300 K (Figure 5d) demonstrates that no organic material was lost during annealing. In addition, the ordering of the multilayer sample as well as the near-planar conformation is robust against such a thermal excitation. This qualifies our method of steering organic layer growth by functionalizing molecules with specific groups as technologically relevant.

2.3. Room Temperature Structure

Para-oligo-phenyl molecules exhibit a phase transformation while cooling from room temperature (RT) to low temperature (~160 K).[54] In the following paragraph, we address the question whether such a phase transition exists also for the functionalized variants. For this purpose we have carried out both X-ray structure analysis and NEXAFS measurements at RT and compared them to the so-far presented data recorded between 160 K and 180 K. In **Figure 8**, we show that the crystal phase at RT is the same as it was for the measurement at reduced temperature. The minor changes are invisible at the scale of the Figures, but appear as small numeric deviations in Table SI 1.

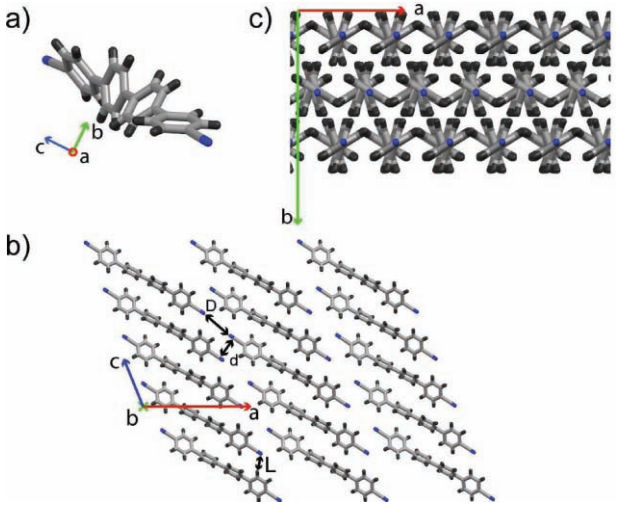

Figure 8. The room-temperature crystal structure of NC–Ph_4–CN as obtained by X-ray structure analysis. (blue = nitrogen, gray = carbon, black = hydrogen) a) The screw-like conformation, b) the chains in the *a*-*c*-plane, c) and the layered packing demonstrated by the view along the long molecular axis are all identical to the situation at low temperatures.

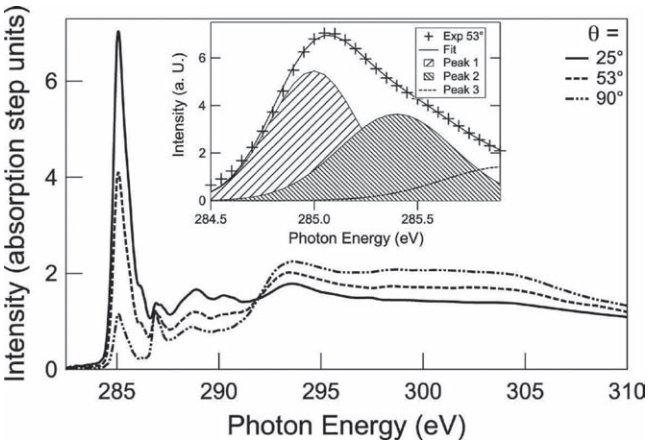

Figure 9. The room temperature NEXAFS signature of OMBE grown thin films of NC–Ph_4–CN shows very similar spectroscopic features compared to the low temperature measurements, with slightly increased peak widths. The twist angle γ-dependent shape (inset) and incidence angle θ-related dichroism of the phenyl related resonance at 285 eV indicate that both the conformation and the packing equals the low temperature case.

The C1s NEXAFS signature of an OMBE grown multilayer sample of NC–Ph_4–CN recorded at RT is depicted in **Figure 9**. The overall spectroscopic structure compares well to the low temperature measurements. The main difference is a slight broadening in the width of the resonances, consistent with the increased thermal excitation. The analysis of the incidence angle θ-related dichroism of the phenyl related resonance at 285 eV indicates that again $\alpha = 25°$. The twist angle γ-dependent shape (inset) was subjected to the same fitting-procedure as the low temperature data, the resulting twist angle amounts to 50°. We conclude that both the conformation and the packing equal the low temperature case.

2.4. Monolayer and Submonolayer Coverage

To understand the origin of the novel uniform packing we investigated the initial growth conditions. Therefore, we carried out a study of the conformation in the monolayer regime. We compared two samples, one with a surface coverage of half a ML and one with a surface coverage of slightly less than one ML. An overview of the comparison is given in **Figure 10**. The STM (scanning tunnelling microscopy) image (Figure 10a) of the 0.5 ML-sample shows the typical open-porous network,[36,55] formed by the NC–Ph_4–CN molecules at temperatures below 200 K. The C1s NEXAFS spectra (Figure 10b) show the typical structure and dichroism as already discussed for the multilayer, but here the spectral features are slightly broadened and shifted to smaller energies by the interaction with the substrate. The angle-dependence of the phenyl peak indicates an angle α of only 15°, thus even smaller than in the multilayer case. In agreement with this, the N1s spectra (Figure 10c) indicate a tilt angle of less than 10°. Since the NEXAFS technique becomes less sensitive for such small angles (see the nearby lying curves for $\alpha = 0°$ and 10° in Figure SI1) and taking into account our error bar, we cannot distinguish signals originating from α

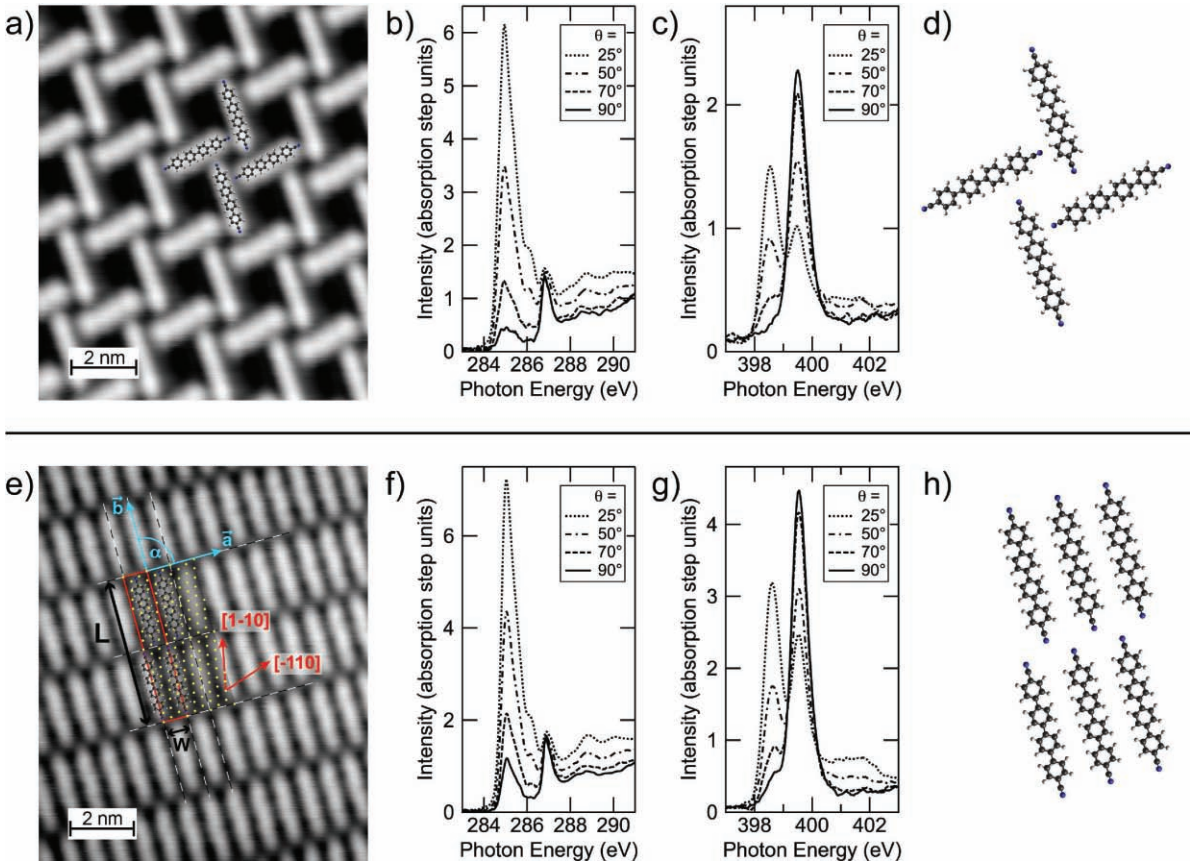

Figure 10. Comparison between a sample with 0.5 ML coverage (a–d) and a sample with 1 ML coverage (e–h). In the submonolayer case, the open-porous network (a: bias voltage V_B = –0.9 V, current I = 85 pA) levels the terminal PhCN-groups into a near-planar arrangement, as evidenced by NEXAFS (b and c) due to the lateral H bonds in the network nodes. In the saturated monolayer case, all molecules are aligned in parallel (e: V_B = –0.2 V, I = 60 pA). NEXAFS indicates a more tilted conformation very near to the multilayer one (f and g). The parallel alignment of the molecules (h) allows tilting of the endgroups due to the missing lateral bonding.

ranging from 0° to 10°. We conclude from the NEXAFS data that the conformation of the molecules in the open-porous network is on average flatter than in the multilayer case. The terminal groups, i.e., the carbonitrile groups together with the first, directly connected phenyl rings, are planar on the surface within the accuracy limits of our setup. The difference in the values of α, as indicated by the C1s region and the N1s region, is explained by the two central phenyl rings being still tilted, to which the N1s region is not sensitive.

For a sample with a surface coverage near to one ML the situation is different. The STM image (Figure 10e) demonstrates the well-ordered dense-packed structure with all molecules in a parallel alignment. This phase can be constructed with an oblique unit cell (red) covering two molecules. From the periodicities (black and white dashed lines) along the molecular rows (direction *a*) and the main axis of the molecules (direction *b*), the experimental values for the dimension of the unit cell are $W = (7.5 \pm 0.2)$ Å, $L = (46.8 \pm 1)$ Å and $\alpha = 91°$. Without having images that simultaneously resolve molecules and atoms, we suggest a commensurate superstructure over the Ag (111) lattice (on-top positions sketched in yellow) based on the fact that we have not seen a Moiré pattern described in matrix notation by $\begin{pmatrix} 3 & -4 \\ -1 & 18 \end{pmatrix}$ with respect to the substrate unit cell vectors [–110] and [1–10]. The unit cell dimensions of the suggested model amount to $W = 7.644$ Å, $L = 47.3$ Å and $\alpha = 91.32°$. Within this primitive cell molecules can be placed such that nitrogen atoms avoid on-top sites. Clearly α is different form the crystal case, suggesting a seed for the growth of the new and differently ordered phase due to the substrate influence. Such a highly regular structure was also reported for a saturated monolayer of sexiphenyldicarbonitrile.[36] For this monolayer structure, the NEXAFS data (Figures 10f and g) indicate a conformation ($\gamma \sim 50°$) very similar to the one in the multilayer case. Note, that the twist angle γ is larger in the monolayer than in the gas phase (free molecule), for which a DFT structure optimization gave $\gamma = 33.5°$.[56] We conclude, that the interaction with the substrate, which should have the tendency to planarize the molecular conformation, is overcompensated by the intermolecular forces of the parallel-aligned species (packing effect) in the dense-packed ML.

The comparison of the results for the submonolayer and the monolayer together leads to the conclusion that the absence of packing constraints and the lateral hydrogen bonds present in the open network (Figure 10d) planarize the terminal groups due to lateral attraction of the phenyl rings. In the case with parallel molecules, this force is not present and the molecules adopt the standard conformation with the rings twisted due to

the steric hindrance of the phenyl rings. This conformation is different from the screw-like bulk conformation due to the influence of the surface. The high order in the saturated layer and the fact that the structure is well explainable with a model based on planar molecules strongly indicate that in this case all the molecules feature β near 0°. Thus, the similarity between the NEXAFS spectra in the saturated monolayer case and the multilayer case further confirms our interpretation that in the multilayer, a uniform alignment of all the molecules is present. The very regular monolayer acts as a high-quality template for the growth of the higher multilayers. The OMBE grown thin films feature uniformly oriented conjugated π systems in contrast to the bulk material and in contrast to OMBE-grown thin films of oligophenyl.

With molecule **4**, we performed an analogous experiment comparing the conformation of the submonolayer structure with the saturated monolayer structure. We have recently reported[36] that molecule **4** also assembles in various open-porous assemblies for the submonolayer case, all of which feature a four-fold binding motif similar to the one displayed in Figure 10d, and that in the saturated layer, the parallel alignment of the molecules is again of the same type as in Figure 10h. The corresponding NEXAFS data (not shown) indicate again that β is approximately 0° and γ is between 40° and 50° in both the monolayer and the multilayer (Figure 5c) case. In comparison to the monolayer, the submonolayer sample is constructed from species with the terminal groups being more planar and with a slightly reduced average phenyl ring tilt. Here, the reduction of the average phenyl angle α is less prominent than for molecule **2**, in full agreement with the fact that for molecule **2** the two terminal groups affected by the lateral H bonds represent half of all phenyl rings while for molecule **4**, only a third of the phenyl rings is affected by the lateral bonds.

We furthermore recorded STM data confirming our interpretation that the molecular conformation is governed by a remarkable ring twist. A sample with approximately 1.5 ML of molecule **4** (**Figure 11**) demonstrates different appearance depending on the layer. Molecules in the first layer (in red) are imaged as stick-like features similar to the appearance in Figure 10. The molecules in the second layer are characterized by distinct intra-molecular features fitting well to the zigzag line observed earlier in a STM study of sexiphenyl on Ag(111).[51] As evidenced by NEXAFS, the twist angle γ is the same in both layers. The appearance of the molecular features is less prominent in the first monolayer due to the interaction with the metal substrate that results in broadening of the molecular levels. With the first layer reducing the influence of the substrate on the second layer, the molecular features appear much more distinct. Similar behavior was discussed in more detail recently.[57]

Our data indicate that along a row (from left–bottom to right–top) all the zigzag features are identical, while from one row to the next the zigzag is inverted (compare solid lines). The regular row-to-row inversion of the zigzag evidences interaction between the rows. Such an interaction can either be direct, for example via the interdigitating carbonitrile groups (cf. Figure 10e), or indirect, for example via the underlying organic layer. We suggest that the twisted geometry of the molecules in the first layer links the geometries of two adjacent rows in the second layer, but a more detailed inspection of this aspect goes beyond the scope of this manuscript. These STM data confirm that neither in the first nor in the second layer any signs are found for the herringbone arrangement typically adopted by the oligophenyl species in which the orientation angles β of adjacent molecules vary by 66°.

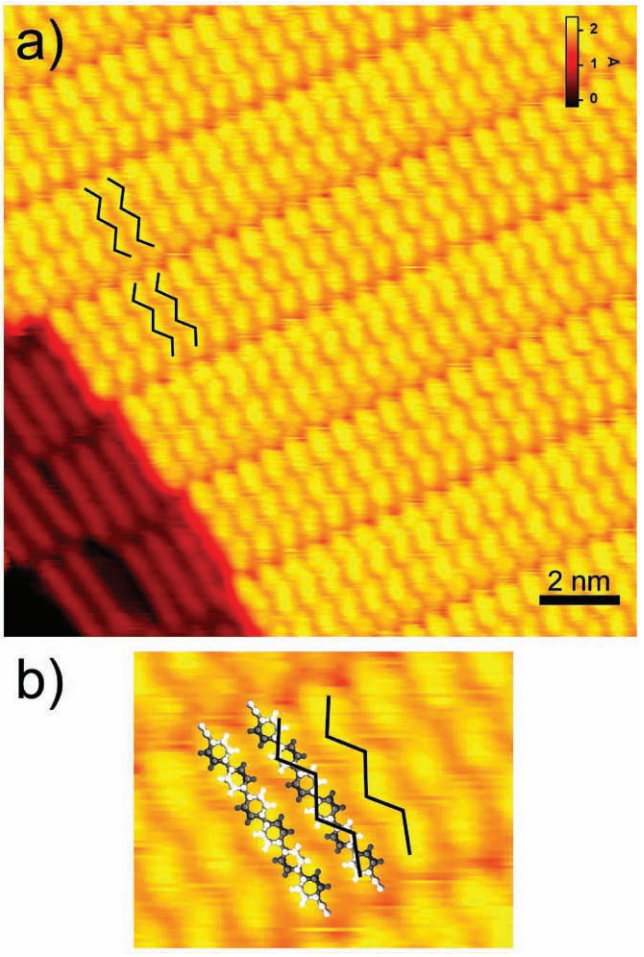

Figure 11. a) STM image (V_B = 1.5 V, I = 60 pA) of a sample with 1.5 monolayer of dicarbonitrile-sexiphenyl (molecule **4**). Molecules in the first layer appear as stick-like protrusions, while for molecules in the second layer, a zigzag-structure can be identified. All molecules show a uniform face-on alignment. b) Enlarged part of the same image as in a). The zigzag-structure (solid line) originates from the rotation of the phenyl rings, alternatively lifting the left and the right side of a phenyl ring (bright atoms) up from the underlying molecular layer.

3. Conclusion

In summary, our study shows that by functionalizing para-oligophenyl molecules with terminal carbonitrile-endgroups at para positions, one can achieve uniform alignment of the conjugated π-systems of the organic thin films. Whereas in the case of the oligophenyls the edge-on face-on packing leads to a mixture of molecular orientations, the functionalized species features uniformly oriented molecules. As an ordering mechanism we suggest a combination of the template effect of the regular first monolayer that consists entirely of face-on

molecules with the promotion of layered growth in multilayers by the functional group. Our study demonstrates a novel method of tuning organic epitaxy and contributes to a better understanding regarding control of thin film properties on the molecular level.

4. Experimental Section

STM: The scanning tunneling microscope (STM) experiments were performed in a UHV system (base pressure in the low 10^{-11} mbar range) equipped with standard sample preparation facilities and a home-built low-temperature STM.[58,59] Images were taken in the constant current mode at approx. 8 K using a W tip. Indicated voltages correspond to sample bias, thus, tunneling takes place from occupied tip states into unoccupied sample states for positive bias. The surfaces were cleaned by repeated ion gun sputtering at room temperature with an Argon flux of approximately 7 μA cm^{-2} and annealing of the Ag crystal to 740 K. The molecules were deposited from a quartz crucible in a Knudsen-type cell held at 450 K, 485 K, 520 K, and 570 K for molecule **1**, **2**, **3**, and **4**, respectively, onto the metal surface at temperatures as indicated. One monolayer (ML) is defined as a molecular adlayer fully covering the surface. NEXAFS measurements were performed at the BESSY II HE-SGM beamline. All spectra were taken at a sample temperature of 160 to 180 K to reduce beam damage.[37] Multilayer spectra were obtained with a slit width of 100 μm corresponding to an energy resolution of approximately 0.2 eV for the C1s edge and 0.3 eV for the N1s edge. Submono and monolayer samples have been studied with a slit width of 200 μm corresponding to an energy resolution of 0.35 eV at the C1s edge. The raw data were treated to concentrate on the adlayer-related information, the details on this data processing are described elsewhere.[60]

Synthesis: Compounds 1–4 were synthesized according to the multistep approach and were published before. (Compound **1**,[61] Compound **2**,**3**,[55,62] Compound **4**[63])

X-ray Structure Determination: Data of **1** and **2** were collected on a STOE IPDS II diffractometer using Mo-Kα radiation ($\lambda = 0.71073$ Å) equipped with a low-temperature device. Structure solution and refinement against F2 were carried out using shelxs and shelxl software.[64] Crystallographic data of **1** and **2** are summarized in Table SI1.

Density Functional Theory: The energy optimized structure of the gas phase molecule of **2** was a zigzag-structure similar to Scheme 2 and obtained in D_2 symmetry with the program package TURBOMOLE at RI–DFT level applying the BP86 functional and a def2-SVP basis set. A helical structure similar to the crystal conformation of **2** was found to be a local energetic minimum, but was slightly higher in energy than the previous one.

The NEXAFS spectra for **2** in zigzag structure were obtained using the program package StoBe.[44] Slaters transition potential method[65,66] was applied in combination with a double basis set technique.[67,68] All basis sets were taken from the StoBe catalog. The core excited carbon atom was equipped with an IGLO III basis set and diffuse basis functions (X-First). The 1s orbital of all other carbon atoms was represented by a pseudo potential combined with a (311/211/1) basis set to ensure a localized core hole. For nitrogen atoms, a (631/21/1) basis set and for hydrogen atoms, a (311/1) basis set were applied. The theoretical spectra were shifted towards lower binding energies by 1.3 eV in order to simplify the comparison with the experimental data.

The molecular geometries with different twist angles γ (from 0° to 60°, Figure 4a) were obtained by rotating the phenyl moieties around the main axis of the optimized zigzag-structure (with $\gamma = 33.5°$) in such a way that the targeted value for γ was achieved. No relaxation of the geometry was carried out in this process.

[Crystallographic data for the compounds **1**, **2** (recorded at 180 K), and **2** (recorded at 293 K) reported in this paper have been deposited with the Cambridge Crystallographic Data Centre as supplementary information publication no. CCDC–752434; 752435; 785057. Copies of the data can be obtained free of charge from www.ccdc.cam.ac.uk/conts/retrieving.html.]

Supporting Information

Supporting Information is available from the Wiley Online Library or from the author.

Acknowledgements

This work was supported by the European Science Foundation Collaborative Research Programme Fun-SMARTs, the TUM Institute of Advanced Studies, the ERC Advanced Grant MolArt, and by the DFG Cluster of Excellence Munich Center for Advanced Photonics. Traveling costs for synchroton measurements provided by the BMBF through Grant No. 05ES3XBA/5 are gratefully acknowledged. K.F. was supported by the Deutsche Forschungsgemeinschaft through the Center for Functional Nanostructures (CFN) in Karlsruhe.

Received: September 15, 2010
Revised: December 17, 2010
Published online: March 11, 2011

[1] R. Resel, *Thin Solid Films* **2003**, *433*, 1.
[2] D. J. Gundlach, Y. Y. Lin, T. N. Jackson, D. G. Schlom, *Appl. Phys. Lett.* **1997**, *71*, 3853.
[3] S. Tasch, C. Brandstätter, F. Meghdadi, G. Leising, G. Froyer, L. Athouel, *Adv. Mater.* **1997**, *9*, 33.
[4] H. Yanagi, S. Okamoto, T. Mikami, *Synth. Met.* **1997**, *91*, 91.
[5] A. Niko, F. Meghdadi, C. Ambrosch-Draxl, P. Vogl, G. Leising, *Synth. Met.* **1996**, *76*, 177.
[6] M. Era, T. Tsutsui, S. Saito, *Appl. Phys. Lett.* **1995**, *67*, 2436.
[7] H. Yanagi, S. Okamoto, *Appl. Phys. Lett.* **1997**, *71*, 2563.
[8] W. Graupner, F. Meghdadi, G. Leising, G. Lanzani, M. Nisoli, S. DeSilvestri, W. Fischer, F. Stelzer, *Phys. Rev. B* **1997**, *56*, 10128.
[9] M. Oehzelt, L. Grill, S. Berkebile, G. Koller, F. P. Netzer, M. G. Ramsey, *ChemPhysChem* **2007**, *8*, 1707.
[10] G. Koller, S. Berkebile, J. R. Krenn, G. Tzvetkov, G. Hlawacek, O. Lengyel, F. P. Netzer, C. Teichert, R. Resel, M. G. Ramsey, *Adv. Mater.* **2004**, *16*, 2159.
[11] Y. Hu, K. Maschek, L. D. Sun, M. Hohage, P. Zeppenfeld, *Surf. Sci.* **2006**, *600*, 762.
[12] J. L. Baudour, H. Cailleau, W. B. Yelon, *Acta Crystallogr. Sect. B-Struct. Commun.* **1977**, *33*, 1773.
[13] J. L. Baudour, Y. Delugeard, P. Rivet, *Acta Crystallogr. Sect. B-Struct. Commun.* **1978**, *34*, 625.
[14] R. Resel, *J. Phys.-Condes. Matter* **2008**, *20*, 184009.
[15] S. Müllegger, I. Salzmann, R. Resel, A. Winkler, *Appl. Phys. Lett.* **2003**, *83*, 4536.
[16] S. Müllegger, K. Hänel, T. Strunskus, C. Wöll, A. Winkler, *Chem Phys Chem* **2006**, *7*, 2552.
[17] Q. Chen, T. Rada, A. McDowall, N. V. Richardson, *Chem. Mater.* **2002**, *14*, 743.
[18] K. Hänel, S. Söhnchen, S. Lukas, G. Beernink, A. Birkner, T. Strunskus, G. Witte, C. Wöll, *J. Mater. Res.* **2004**, *19*, 2049.
[19] D. Käfer, L. Ruppel, G. Witte, *Phys. Rev. B* **2007**, *75*, 085309.
[20] D. Käfer, G. Witte, *Chem. Phys. Lett.* **2007**, *442*, 376.
[21] S. Söhnchen, S. Lukas, G. Witte, *J. Chem. Phys.* **2004**, *121*, 525.
[22] G. Witte, C. Wöll, *J. Mater. Res.* **2004**, *19*, 1889.
[23] G. Witte, C. Wöll, *Phys. Status Solidi A* **2008**, *205*, 497.

[24] F. S. Tautz, S. Sloboshanin, V. Shklover, R. Scholz, M. Sokolowski, J. A. Schaefer, E. Umbach, *Appl. Surf. Sci.* **2000**, *166*, 363.
[25] F. Klappenberger, M. E. Cañas-Ventura, S. Clair, S. Pons, U. Schlickum, Z. R. Qu, T. Strunskus, A. Comisso, C. Wöll, H. Brune, K. Kern, A. DeVita, M. Ruben, J. V. Barth, *ChemPhysChem* **2008**, *9*, 2522.
[26] M. Oehzelt, S. Berkebile, G. Koller, J. Ivanco, S. Surnev, M. G. Ramsey, *Surf. Sci.* **2009**, *603*, 412.
[27] P. Ruffieux, O. Gröning, M. Bielmann, C. Simpson, K. Müllen, L. Schlapbach, P. Gröning, *Phys. Rev. B* **2002**, *66*, 073409.
[28] J. Stöhr, *NEXAFS Spectroscopy and the Structure of Molecules Bonded to Surfaces*, Springer, **1991**.
[29] D. Britton, V. G. Young, *Acta Crystallogr., Sect. E: Struct. Rep. Online* **2003**, *59*, 1849.
[30] C. Janiak, *J. Chem. Soc., Dalton Trans.* **2000**, 3885.
[31] K. S. Min, M. P. Suh, *Eur. J. Inorg. Chem.* **2001**, 449.
[32] Y. L. Wang, Q. Y. Liu, L. Xu, *Acta Crystallogr., Sect. C: Cryst. Struct. Commun.* **2007**, *63*, 304.
[33] C. J. Clews, E. N. Maslen, H. M. Rietveld, *Nature* **1961**, *192*, 154.
[34] P. J. Low, M. A. J. Paterson, A. E. Goeta, D. S. Yufit, J. A. K. Howard, J. C. Cherryman, D. R. Tackley, B. Brown, *J. Mater. Chem.*, 2516.
[35] A. Moser, O. Werzer, H. G. Flesch, M. Koini, D. M. Smilgies, D. Nabok, P. Puschnig, C. Ambrosch-Draxl, M. Schiek, H. G. Rubahn, R. Resel, *Eur. Phys. J. Spec. Top.* **2009**, *167*, 59.
[36] D. Kühne, F. Klappenberger, R. Decker, U. Schlickum, H. Brune, S. Klyatskaya, M. Ruben, J. V. Barth, *J. Phys. Chem. C* **2009**, *113*, 17851.
[37] P. Feulner, T. Niedermayer, K. Eberle, R. Schneider, D. Menzel, A. Baumer, E. Schmich, A. Shaporenko, Y. Tai, M. Zharnikov, *Phys. Rev. Lett.* **2004**, *93*, 178302.
[38] P. J. Cumpson, *Surf. Interface Anal.* **2001**, *31*, 23.
[39] D. Duflot, J. P. Flament, J. Heinesch, M. J. Hubin-Franskin, *J. Electron Spectrosc. Relat. Phenom.* **2000**, *113*, 79.
[40] R. Püttner, C. Kolczewski, M. Martins, A. S. Schlachter, G. Snell, M. Sant'Anna, J. Viefhaus, K. Hermann, G. Kaindl, *Chem. Phys. Lett.* **2004**, *393*, 361.
[41] S. Carniato, V. Ilakovac, J. J. Gallet, E. Kukk, Y. Luo, *Phys. Rev. A* **2005**, *71*, 022511.
[42] T. Strunskus, V. Staemmler, K. Fink, K. Diller, F. Klappenberger, J. V. Barth, C. Wöll, unpublished.
[43] J. X. Liu, B. Schupbach, A. Bashir, O. Shekhah, A. Nefedov, M. Kind, A. Terfort, C. Wöll, *Phys. Chem. Chem. Phys.* **2010**, *12*, 4459.
[44] K. Hermann, L. G. M. Pettersson, StoBe-deMon version 3.0, **2009**.
[45] K. Fink, T. Bodenstein, K. Diller, F. Klappenberger, J. V. Barth, V. Staemmler, C. Wöll, unpublished.
[46] C. Ambrosch-Draxl, J. A. Majewski, P. Vogl, G. Leising, *Phys. Rev. B* **1995**, *51*, 9668.
[47] J. L. Baudour, Y. Delugeard, H. Cailleau, *Acta Crystallogr., Sect. B: Struct. Commun.* **1976**, *32*, 150.
[48] Y. Delugeard, J. Desuche, J. L. Baudour, *Acta Crystallogr., Sect. B: Struct. Commun.* **1976**, *32*, 702.
[49] J. L. Baudour, *Acta Crystallogr., Sect. B: Struct. Commun.* **1991**, *47*, 935.
[50] C. Ambrosch-Draxl, P. Puschnig, R. Resel, G. Leising, *Synth. Met.* **1999**, *101*, 673.
[51] K. F. Braun, S. W. Hla, *Nano Lett.* **2005**, *5*, 73.
[52] S. Guha, W. Graupner, R. Resel, M. Chandrasekhar, H. R. Chandrasekhar, R. Glaser, G. Leising, *Phys. Rev. Lett.* **1999**, *82*, 3625.
[53] S. Guha, W. Graupner, R. Resel, M. Chandrasekhar, H. R. Chandrasekhar, R. Glaser, G. Leising, *Synth. Met.* **1999**, *101*, 180.
[54] K. N. Baker, A. V. Fratini, T. Resch, H. C. Knachel, W. W. Adams, E. P. Socci, B. L. Farmer, *Polymer* **1993**, *34*, 1571.
[55] U. Schlickum, R. Decker, F. Klappenberger, G. Zoppellaro, S. Klyatskaya, W. Auwärter, S. Neppl, K. Kern, H. Brune, M. Ruben, J. V. Barth, *J. Am. Chem. Soc.* **2008**, *130*, 11776.
[56] TURBOMOLE version 6.0, 2008, TURBOMOLE GmbH, Karlsruhe (Germany), www.turbomole.com (accessed February, 2011).
[57] I. Fernandez-Torrente, K. J. Franke, J. I. Pascual, *J. Phys.-Condes. Matter* **2008**, *20*, 184001.
[58] S. Clair, Ph. D. Thesis, Ecole Polytechnique Fédérale de Lausanne, Lausanne **2004**.
[59] S. Clair, S. Pons, A. P. Seitsonen, H. Brune, K. Kern, J. V. Barth, *J. Phys. Chem. B* **2004**, *108*, 14585.
[60] M. E. Cañas-Ventura, F. Klappenberger, S. Clair, S. Pons, K. Kern, H. Brune, T. Strunskus, C. Wöll, R. Fasel, J. V. Barth, *J. Chem. Phys.* **2006**, *125*, 184710.
[61] J. Colonge, J. Buedina, J. Sabadie, *Bull. Soc. Chim. Fr.* **1967**, 4370.
[62] U. Schlickum, R. Decker, F. Klappenberger, G. Zoppellaro, S. Klyatskaya, M. Ruben, I. Silanes, A. Arnau, K. Kern, H. Brune, J. V. Barth, *Nano Lett.* **2007**, *7*, 3813.
[63] D. Kühne, F. Klappenberger, R. Decker, U. Schlickum, H. Brune, S. Klyatskaya, M. Ruben, J. V. Barth, *J. Am. Chem. Soc.* **2009**, *131*, 3881.
[64] G. M. Sheldrick, SHELXTL–97, Program for the Refinement of Crystal Structures, **1997**.
[65] J. C. Slater, K. H. Johnsen, *Phys. Rev. B* **1972**, *5*, 844.
[66] J. C. Slater, *Adv. Quant. Chem.* **1972**, *6*, 1.
[67] L. Triguero, L. G. M. Pettersson, H. Ågren, *J. Phys. Chem. A* **1998**, *102*, 10599.
[68] L. Triguero, L. G. M. Pettersson, H. Ågren, *Phys. Rev. B* **1998**, *58*, 8097.